

Observations of a pulse driven cool polar jet by SDO/AIA

Abhishek Kumar Srivastava^{1,2} and Kris Murawski²

¹ Aryabhata Research Institute of Observational Sciences (ARIES), Manora Peak, Nainital-263 129, Uttarakhand, India

e-mail: aks@aries.res.in

² Group of Astrophysics, UMCS, ul. Radziszewskiego 10, 20-031 Lublin, Poland

e-mail: kmur@kft.umcs.lublin.pl

Received / Accepted

ABSTRACT

Context. We observe a solar jet at north polar coronal hole (NPCH) using SDO AIA 304 Å image data on 3 August 2010. The jet rises obliquely above the solar limb and then retraces its propagation path to fall back.

Aims. We numerically model this observed solar jet by implementing a realistic (VAL-C) model of solar temperature.

Methods. We solve two-dimensional ideal magnetohydrodynamic equations numerically to simulate the observed solar jet. We consider a localized velocity pulse that is essentially parallel to the background magnetic field lines and initially launched at the top of the solar photosphere. The pulse steepens into a shock at higher altitudes, which triggers plasma perturbations that exhibit the observed features of the jet. The typical direction of the pulse also clearly exhibits the leading front of the moving jet.

Results. Our numerical simulations reveal that a large amplitude initial velocity pulse launched at the top of the solar photosphere produces in general the observed properties of the jet, e.g., upward and backward average velocities, height, width, life-time, and ballistic nature.

Conclusions. The close matching between the jet observations and numerical simulations provides first strong evidence for the formation of this jet by a single velocity pulse. The strong velocity pulse is most likely generated by the low-atmospheric reconnection in the polar region which results in triggering of the jet. The downflowing material of the jet most likely vanishes in the next upcoming velocity pulses from lower solar atmosphere, and therefore distinctly launched a single jet upward in the solar atmosphere is observed.

Key words. Magnetohydrodynamics (MHD) – Sun: atmosphere– Sun : corona

1. Introduction

Solar jets are the typical collimated and short lived transient ejecta in the solar atmosphere that are significant in mass and energy transport at short spatio-temporal scales. Based on the spatial sizes, life times, and transient nature, the jets are classified in the form of various phenomena, e.g., anemone jets (Shibata et al. 2007), EUV jets (Innes et al. 1997), spicules (Bohlin et al. 1975), X-ray jets (Shibata et al. 1992), and penumbral jets (Katsukawa et al. 2007). The solar surges are cool jets typically formed with a plasma usually evident in H α and other chromospheric lines, and they are supposed to be triggered by magnetic reconnection processes (Brooks et al. 2007). However, solar surges are mostly associated with the flaring regions and the places of transient activities at the Sun. Georgakilas et al. (1999) have also observed the polar surges which were the cool surge-like jets over polar caps formed without any transient phenomenon. However, they were having association with macro-spicules, and due to the short-lived nature they could not attain the greater heights in off-limb polar corona.

Other short spatio-temporal scale jets (e.g., dynamic fibrils, mottles, and spicules) are also significant low-atmospheric phenomena to understand its energy and mass transport. Using high-resolution observations from 1 m Swedish Solar Telescope and advanced numerical modeling, Hansteen et al. (2006) have shown that in the active

regions these jets are a natural consequence of upwardly propagating slow-mode magnetoacoustic shocks generated due to the leakage of p-mode sub-photospheric oscillations. The active region fibrils are also most likely formed by chromospheric shock waves that occur when convective flows and global oscillations leak into the chromosphere along the field lines of magnetic flux concentrations (De Pontieu et al. 2007a). De Pontieu et al. (2004) have also reported for the first time the quasi-periodic rise and fall of the spicule material due to the leakage of p-mode oscillations from the sub-photospheric regions. De Pontieu et al. (2007b) have pointed out that typical type-I spicules are found to be driven by shock waves that form when global oscillations and convective flows leak into the upper atmosphere along magnetic field lines on 3-7 minute timescales. They have also found the signature of type-II spicules, which are much more dynamically formed within 10 s and are very thin (200 km wide) with the lifetimes of 10-150 s. These type of spicules seem to be rapidly heated to transition region temperatures and eject material through the chromosphere at speeds of 50-150 km s⁻¹. The properties of Type II spicules suggest a formation process that is a consequence of magnetic reconnection, typically in the vicinity of magnetic flux concentrations in plage and network regions. Recently, Morton et al. (2011) have reported a unique signature of the relationship between spicule-like structures and the polar jet formation using the SDO/AIA observations. However,

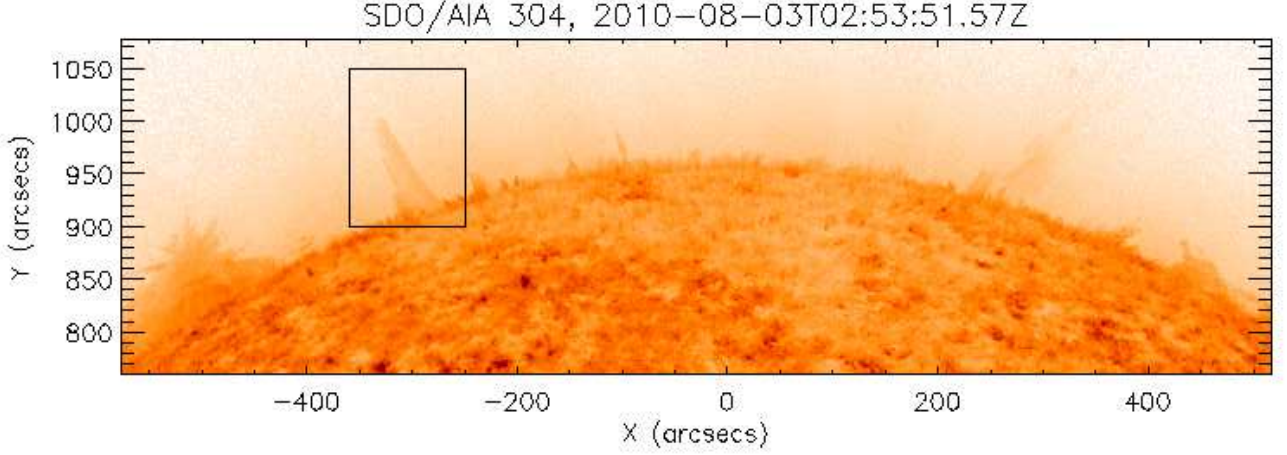


Fig. 1. The field-of-view of the north polar coronal hole (NPCH) as observed by SDO/AIA 304 Å on 03 August 2010 at 02:53:51 UT. The (X_{cen}, Y_{cen}) was $(-29.618'', 918.631'')$, while the full FOV was $(1094'', 317'')$ wide with a resolution of $0.6''$ per pixel. The black box shows the triggering of a solar jet that exhibits an exceptional phenomena of its most probable formation by a velocity pulse.

the relationships between various types of jets are still not well explored.

In various types of these jet phenomena, the coronal and polar coronal jets are very classic transient phenomena that have been observed from Skylab and Yohkoh era in soft X-rays (Shimojo & Shibata 2000), followed by Solar and Heliospheric Observatory (SoHO) (Wang et al. 1998), Transition Region and Coronal Explorer (TRACE) (Alexander & Fletcher 1999), and Hinode (Kamio et al. 2007; Filippov et al. 2009). The magnetic reconnection is found to be one of the most likely mechanisms for the generation of typical coronal jets (Shibata et al. 2007), while the reconnection generated waves may also be present with the jets during their propagation (Yokoyama & Shibata 1995, 1996). Pariat et al. (2009) have recently simulated the propagation of kink motion along the magnetic field lines around a rotating and closed magnetic field region. This dynamics is most likely associated with the kink instability in the jet formation region, which may lead its upward motion in the model solar atmosphere. The transversal waves have also been recently detected in association with the solar jet events at small spatial scales (e.g., He et al. 2009; Kamio et al., 2010, and references cited there). However, the evidence of Alfvén waves has also been detected in the large-scale polar X-ray jets (Cirtain et al., 2007). Therefore, the magnetic reconnection and associated waves may be the most likely drivers to energize such type of the jets at various spatio-temporal scales. However, the exact mechanism is not well established in the context of the very complex motion of the various types of solar jets.

Recently, Murawski & Zaqarashvili (2010) have reported the formation of solar spicules by a pulse launched within the chromosphere. Their numerical simulations show that the strong initial pulse may lead to the quasi-periodic rising of the chromospheric material into the lower corona in the form of spicules. They have explained the observed speed, width, and heights of type I spicules, as well as observed multi-structural and bi-directional flows with a quasi-periodic rise and fall at 3-5 min time scales due to the consecutive shocks. The reconnection generated veloc-

ity pulses may also drive the solar jets. However, such models along with their observational supports are not yet available in the context of solar jets. Therefore, it may be worth to explore the launching of solar jet due to the formation of a pulse in the lower solar atmosphere.

In the present paper, we find a unique observational signature of a jet in the north polar coronal hole which shows its dynamics as driven by a velocity pulse. We numerically simulate the similar kind of jet triggered by a strong amplitude velocity pulse in the lower solar atmosphere, which in general closely mimics the observed properties of the jet. In Sec 2, we describe the observational data and analyses. We report the numerical model in Sec 3, and results of numerical simulation in Sec 4. We present the discussion and conclusions in the last section.

2. Observations and results

We use a time-series data of a solar jet at north polar coronal hole as observed in 304 Å filter of Atmospheric Assembly Imager (AIA) onboard the Solar Dynamics Observatory (SDO) on 3 August 2010 during 02:41:14 UT–03:02:50 UT. The SDO/AIA has a typical resolution of $0.6''$ per pixel and the highest cadence of 12 s, and it observes the full solar disk in three UV (1600 Å, 1700 Å, 4500 Å) and seven EUV (171 Å, 193 Å, 211 Å, 94 Å, 304 Å, 335 Å, 131 Å) wavelengths (Lemen et al. 2011). Therefore, it provides the unprecedented observations of multi-temperature, high-resolution, and high-temporal plasma dynamics all over the Sun. The field-of-view of the north polar coronal hole as observed by SDO/AIA 304 Å on 03 August 2010 at 02:53:51 UT is shown in Fig. 1. The (X_{cen}, Y_{cen}) was $(-29.618'', 918.631'')$, while the full FOV was $(1094'', 317'')$ wide with the resolution of $0.6''$ per pixel. The black box shows the triggering of a solar jet off the polar limb. The time series has been obtained by the SSW cutout service at LMSAL, USA, which is corrected for the flat-field and spikes. We run `aia_prep` subroutine of SSW IDL also for further calibration and cleaning of the time series data.

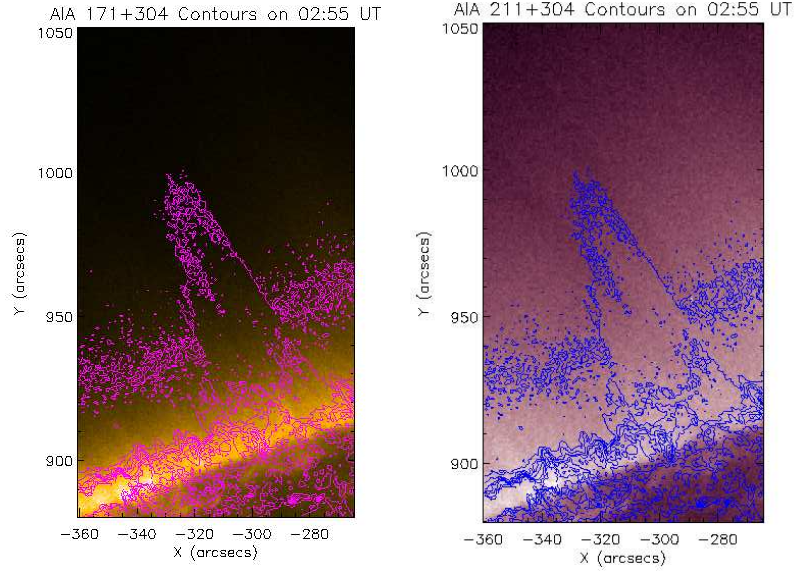


Fig. 2. The SDO/AIA 171 Å (left) and 211 Å (right) coronal images overlaid by SDO/AIA 304 Å intensity contours. It is clearly evident that the coronal filters does not reveal any sensitivity to the jet plasma, which is observed in the He II 304 Å filter.

We observe a very unique jet formation in the east-north limb of the polar coronal hole, which seems to be driven by a velocity pulse launched in the lower solar atmosphere. The jet has been launched slightly obliquely from the background open field lines of the polar coronal hole (cf., Fig. 2). The life-time of the jet was observed as ~ 21 min, which is the typical life time of the coronal jets previously observed in the Sun and cataloged by Nisticó et al. (2009). We observe a typical jet that reaches in the corona off the polar limb. However, the jet material was only visible in He II 304 Å filter, which is sensitive to the comparatively cool temperature of 1×10^5 K. The jet material could not be evident in the typical TR/coronal filters (e.g., Fe IX 171 Å, 211 Å filters) of SDO/AIA, which are sensitive to the plasma temperature $\geq 10^6$ K. Fig. 2 shows the SDO/AIA 171 Å (left) and 211 Å (right) coronal images overlaid by SDO/AIA 304 Å intensity contours at a time of the maximum rise of the jet. It is clearly evident that the coronal filters do not exhibit any sensitivity to the jet plasma, which is only observed in the He II 304 Å filter. This scenario persist during whole life-time of the observed jet. The unique jet is a very faint event even captured in 304 Å as most of the strong emissions come from spicule borders at this wavelength also. However, we may not rule out some very weak amount of coronal emissions also that could not be distinguished in the diffused background off the polar limb. Therefore, we abbreviate this jet as a cool jet as its plasma mostly emits the radiations captured by the AIA filters that are sensitive to cooler plasma emissions, e.g., 304 Å. There may also be the possibility of some traces of emissions in other SDO/AIA filters (e.g., 1600 Å) that are sensitive to the emissions from comparatively cooler plasma. This means that the jet material was typically formed by comparatively cooler plasma compared to the background coronal plasma, and it moves in form of plasma column that does not exchange any heat with the ambient coronal plasma. This was the unique property of the observed cool jet off-limb in the polar coronal hole. Our observed cool ejecta reaches at a higher height (72 Mm) with a life-time

of 21 min and larger width of 20 Mm. We, therefore, abbreviate it as a cool polar jet, rather as an evidence of any polar surge like ejecta.

The jet starts moving up above the solar limb on $\sim 02:41$ UT and reaches at a maximum height of ~ 72 Mm at 02:52 UT. Therefore, its average rising speed is ~ 110 km s $^{-1}$ that is the typical speed of the jet by which it rose in the corona at a maximum height of ~ 72 Mm in the first ~ 648 s of the time (Fig. 3). Although, the width slightly varies during the course of time at the base of the jet, its shape is approximately uniform during its rise-up. Its width at the base is measured approximately as ~ 20 Mm. The unique evidence this jet presented is its rise straight in the corona off-limb in first 10-11 min of its life time, and then its fall back from the same path in rest of the duration of its life time. Some unique observations of chromospheric jet by Hinode/SOT Ca II H filter revealed fine structuring as well as transversal motion that was associated with the helicity injection in the upper solar atmosphere (Liu et al. 2009). However, the spatial resolution of SDO/AIA (0.6'') is indeed lower compared to SOT (0.2''), and secondly the observed cool jet is very fainter to clearly identify such fine structuring. Moreover, the observed intriguing chromospheric jet (Liu et al. 2009) was associated with a small flare at the western limb, while in the present case we observe the cool jet in polar coronal hole. Therefore, these two cases are entirely different, and we do not observe such type of oscillating threads as well as helicity injection in our observations.

The similar type of the dynamics in form of the parabolic trajectory has been reported in case of various types of spicules (type I and II), dynamic fibrils, mottles (Hansteen et al. 2006; De Pontieu et al. 2007a,b, 2011). These findings also support the acceleration of such small-scale jets by the shock triggered in the chromosphere due to velocity pulses generated by the leakage of sub-photospheric p-modes. However, such drivers need few km s $^{-1}$ velocity amplitude, 3-5 minutes temporal scales, as well as some concentrated field regions of few hundred Gauss to push such jets 2-10 Mm above the solar limb. Recently, Murawski & Zaqarashvili (2010) have also simulated the solar spicules

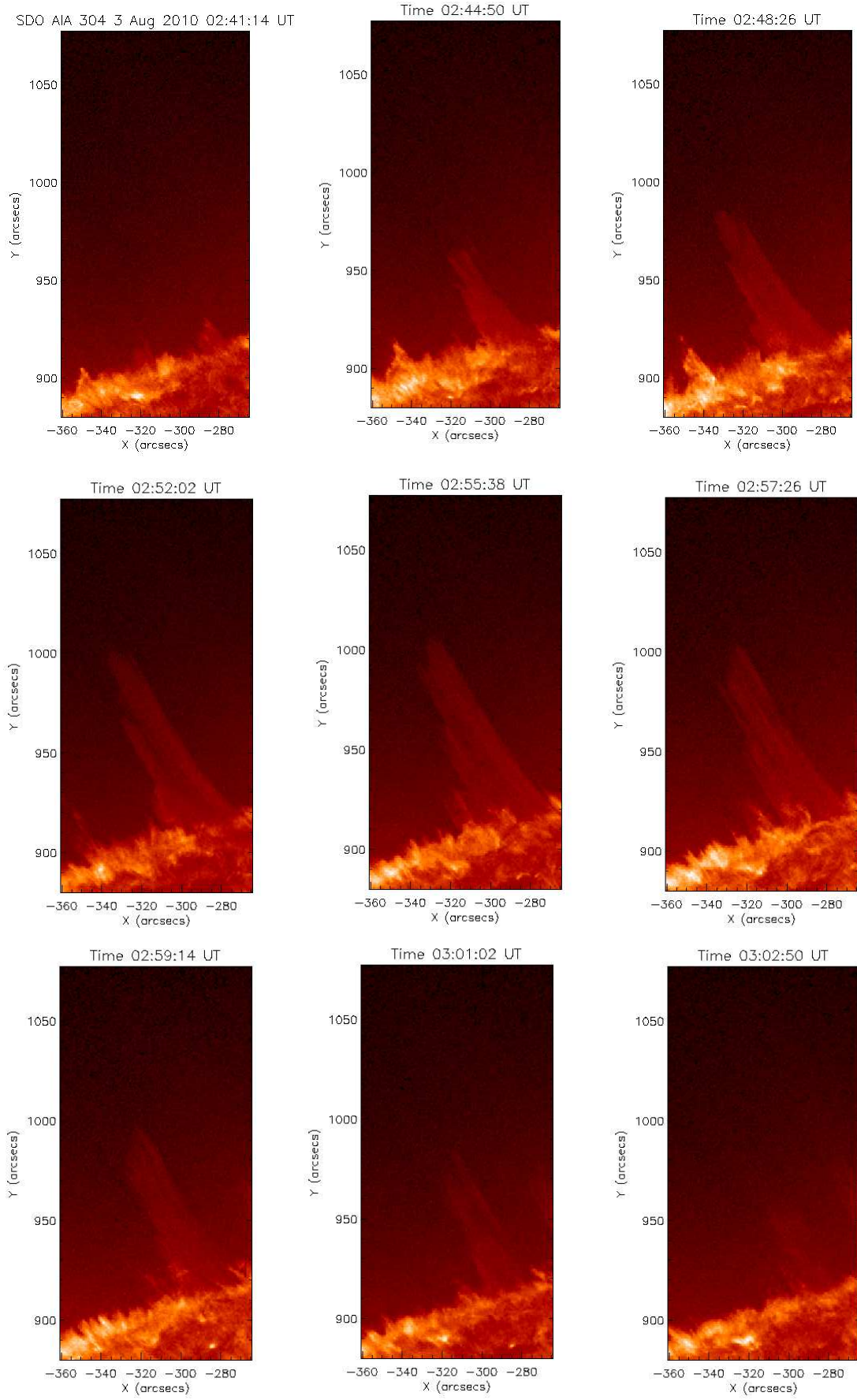


Fig. 3. The SDO/AIA 304 Å time sequence of a cool jet propagation above the solar limb in the north-east polar coronal hole that clearly shows the upward motion of the plasma and its downward motion along the same path.

by launching a velocity pulse above the solar photosphere. However, the strong velocity pulse will be needed in the present case to trigger a jet material higher in the corona.

Our observed dynamics supports that this jet may also be formed by a velocity pulse that triggered in the chromosphere and steepens in form of a shock in the transition region/corona. However, it may not be associated with typical photospheric velocity pulses of the order of few km s⁻¹ associated with the leakage of p-modes that launches the small-scale jets as mentioned in many significant previous studies (Hansteen et al. 2006; De Pontieu et al. 2007a,b). In the present case, the steepened shock can be generated by a reconnection generated strong velocity pulse. Its front may rarefy the plasma density behind it, and the jet plasma could move up. After reaching in the corona along a curved magnetic field lines, this jet falls back due to gravity and cool plasma traced back its backward path as observed here. In next section, we discuss in details the numerical simulation of the observed jet in the solar atmosphere triggered by a strong velocity pulse.

3. A numerical model

Our model system is taken to be composed of a gravitationally-stratified solar atmosphere which is described by the ideal two-dimensional (2D) MHD equations:

$$\frac{\partial \rho}{\partial t} + \nabla \cdot (\rho \mathbf{V}) = 0, \quad (1)$$

$$\rho \frac{\partial \mathbf{V}}{\partial t} + \rho (\mathbf{V} \cdot \nabla) \mathbf{V} = -\nabla p + \frac{1}{\mu} (\nabla \times \mathbf{B}) \times \mathbf{B} + \rho \mathbf{g}, \quad (2)$$

$$\frac{\partial p}{\partial t} + \nabla \cdot (p \mathbf{V}) = (1 - \gamma) p \nabla \cdot \mathbf{V}, \quad (3)$$

$$\frac{\partial \mathbf{B}}{\partial t} = \nabla \times (\mathbf{V} \times \mathbf{B}), \quad \nabla \cdot \mathbf{B} = 0. \quad (4)$$

Here ρ is mass density, \mathbf{V} is flow velocity, \mathbf{B} is the magnetic field, $p = \frac{k_B}{m} \rho T$ is gas pressure, T is temperature, $\gamma = 5/3$ is the adiabatic index, $\mathbf{g} = (0, -g)$ is gravitational acceleration of its value $g = 274 \text{ m s}^{-2}$, m is mean particle mass and k_B is the Boltzmann's constant.

3.1. Equilibrium configuration

We assume that at its equilibrium the solar atmosphere is still ($\mathbf{V}_e = 0$) with a force-free magnetic field,

$$(\nabla \times \mathbf{B}_e) \times \mathbf{B}_e = 0, \quad (5)$$

such that it satisfies a current-free condition, $\nabla \times \mathbf{B}_e = 0$, and it is specified by the magnetic flux function, A , as

$$\mathbf{B}_e = \nabla \times (A \hat{\mathbf{z}}).$$

Here the subscript _e corresponds to equilibrium quantities. We set an arcade magnetic field by choosing

$$A(x, y) = B_0 \Lambda_B \cos(x/\Lambda_B) \exp[-(y - y_r)/\Lambda_B]. \quad (6)$$

Here, B_0 is the magnetic field at $y = y_r$, and the magnetic scale-height is

$$\Lambda_B = 2L/\pi. \quad (7)$$

We set and hold fixed $L = 100 \text{ Mm}$.

As a result of Eq. (5) the pressure gradient is balanced by the gravity force,

$$-\nabla p_e + \rho_e \mathbf{g} = 0. \quad (8)$$

With a use of the ideal gas law and the y -component of Eq. (8), we arrive at

$$p_e(y) = p_0 \exp \left[- \int_{y_r}^y \frac{dy'}{\Lambda(y')} \right], \quad \rho_e(y) = \frac{p_e(y)}{g \Lambda(y)}, \quad (9)$$

where

$$\Lambda(y) = k_B T_e(y) / (mg) \quad (10)$$

is the pressure scale-height, and p_0 denotes the gas pressure at the reference level that we choose in the solar corona at $y_r = 10 \text{ Mm}$.

We adopt an equilibrium temperature profile $T_e(z)$ for the solar atmosphere that is close to the VAL-C atmospheric model of Vernazza et al. (1981). Then with the use of Eq. (9) we obtain the corresponding gas pressure and mass density profiles.

3.2. Perturbations

We initially perturb the above equilibrium impulsively by a Gaussian pulse in the vertical component of velocity, V_y , viz.,

$$V_y(x, y, t = 0) = A_v \exp \left[- \frac{(x - x_0)^2}{w_x^2} - \frac{(y - y_0)^2}{w_y^2} \right]. \quad (11)$$

Here A_v is the amplitude of the pulse, (x_0, y_0) is its initial position and w_x, w_y denote its widths along the x - and y -directions, respectively. We set and hold fixed $A_v = 160 \text{ km s}^{-1}$, $x_0 = -17.5 \text{ Mm}$, $y_0 = 1.75 \text{ Mm}$, $w_x = 10 \text{ Mm}$, and $w_y = 0.1 \text{ Mm}$.

4. Results of numerical simulations

Equations (1)-(4) are solved numerically using the code FLASH (Lee & Deane 2009). This code implements a second-order unsplit Godunov solver with various slope limiters and Riemann solvers, as well as adaptive mesh refinement (AMR). We set the simulation box of $(-125, 15) \text{ Mm} \times (0, 110) \text{ Mm}$ along the x - and y -directions and impose fixed in time all plasma quantities at all four boundaries of the simulation region. In all our studies we use AMR grid with a minimum (maximum) level of refinement set to 4 (8). The refinement strategy is based on controlling numerical errors in mass density, which results in an excellent resolution of steep spatial profiles and greatly reduces numerical diffusion at these locations.

Figure 4 displays the spatial profiles of plasma temperature (colour maps) and velocity (arrows) resulting from the initial velocity pulse of Eq. (11), which splits into counter-propagating parts. The part which propagates downwards becomes reflected from the dense plasma layers at the photospheric region. This reflected part lags behind the originally upward propagating signal which becomes a shock. As the plasma is initially pushed upwards the under-pressure results in the region below the initial pulse. This under-pressure sucks up comparatively cold chromospheric plasma which lags behind the shock front at higher temperature.

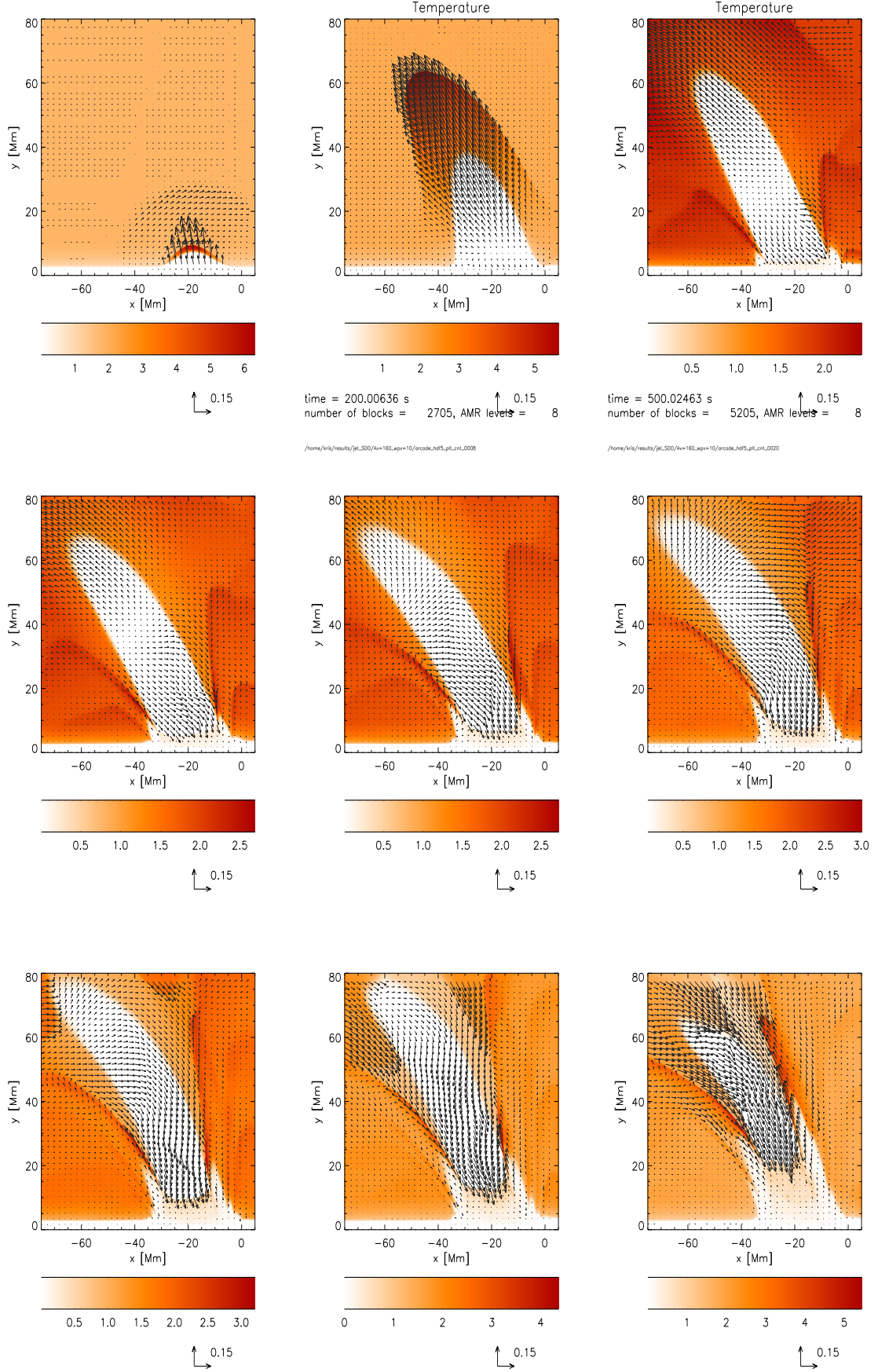


Fig. 4. Temperature (colour maps) and velocity (arrows) profiles at $t = 25$ s, $t = 200$ s, $t = 500$ s, $t = 600$ s, $t = 700$ s, $t = 800$ s, $t = 900$ s, $t = 1000$ s, and $t = 1200$ s (from top-left to bottom-right). Temperature is drawn in units of 1 MK. The arrow below each panel represents the length of the velocity vector, expressed in units of 150 km s^{-1} .

As a result, the pressure gradient force works against gravity and forces the chromospheric material to penetrate into the solar corona in form of rarefaction wave. At $t = 25$ s this shock reaches the altitude of $y \simeq 10$ Mm and the rarefaction wave is located 1 Mm below the slow shock. The next snapshot (top middle panel) is drawn for $t = 200$ s. At this time the slow shock reached the altitude of $y \simeq 63$ Mm while the chromospheric plasma is located below at $y \simeq 40$ Mm. At the next moment of time, $t = 500$ s, (top right panel) the shock moved up and the chromospheric plasma blob exhibits its developed phase, reaching the level of $y = 64$ Mm, which matches well with the observational data of Fig. 3(top right panel). The cool jet slow down while propagating upwards. At $t = 800$ s it arrived at the level of $y \simeq 70$ Mm (Fig.3, middle-right panel) and subsequently subsided as the plasma began to flow downward, being attracted by gravity (bottom panels). At the subsiding stage the fine structures developed as a result of interaction between falling down plasma and rising up secondary pulse. Similar features were evident in the case of the numerical simulation of spicules (Murawski & Zaqarashvili 2010).

5. Discussions and Conclusion

Our numerical simulations show a general scenario of rising and subsequently falling down cool plasma jet with a number of observational features like jet height and width, ballistic motion, approximate rising time-scale and average rising velocity that are being close to the observational data. However, some match between the numerical and observational data is approximate and rather qualitative, e.g., the rising time-scale in the simulation is ~ 800 s while in the real observations it is ~ 720 s. This mismatch may obviously result from some of the simplified profiles of the model parameters in our developed numerical model, e.g., the magnetic field configuration at a place at which the initial pulse was launched, and so on. Moreover, the real jet was excited in more complex plasma and magnetic field conditions at the polar coronal hole of the Sun. We might not model exactly realistically the way in which the jet was excited in the real Sun. In fact, the exciter could work for some time, it could be located at a different place and it could have a different size, speed and distribution. As such data is not provided by the observations we decided to trigger the jet by a localized pulse in a plasma velocity, that is launched below the transition region. By this way we managed to excite the jet which mimics on average the properties of the observed cool plasma jet. The small mismatches like the exact height and length of the jet as well as its descending time can be reduced by tuning of free parameters in the numerical model. In particular, the jet length would be smaller for a smaller amplitude of the initial pulse. We did not expect to fit perfectly our numerical data to the observational findings but instead our intention was to show a qualitative and to some extent quantitative agreement between the numerical and observational approaches.

It is noteworthy that recently Culhane et al. (2007) have found the first observational evidence of unique EUV polar jets which could not escape from the Sun as like the jets previously observed with SXT in Yohkoh era. They conject that such accelerated polar jet plasma is being heated upto coronal temperature with its rise, and then fall back to lower atmosphere after its cooling. They observed jet velocities in the range of 150 km s^{-1} - 360 km s^{-1} and reported

their formation most probably due to the magnetic reconnection between emerging bipoles with the large-scale open field lines of the polar coronal hole. Ko et al. (2005) have also found cool and hot plasma components in a limb jet, as well as its falling back scenario in the lower atmosphere. However, all these previously observed jets were found to be consistent with the impulsive transient heating (e.g., as driven by direct reconnection processes), and thereafter cooling and draining along the same path. We also observe the jet motion that moves up and thereafter falls along the same path in the lower atmosphere. However, the jet is made by the cool plasma maintained at a temperature of $\sim 10^5$ K, which is sensitive to the SDO/AIA 304 Å filter representing upper chromospheric/TR plasma. However, the jet plasma column is not evident at typical coronal temperature of 1.0 MK in the SDO/AIA 171 Å. Therefore, the jet consists of a cool plasma even after reaching at the coronal heights, and does not subject to any heating and cooling events as previously observed by Culhane et al. (2007); Ko et al. (2005). The primary mechanism for the origin of such jet may be the magnetic reconnection between the emerging bipolar magnetic fields and pre-existing open field lines in the polar coronal hole (Culhane et al. 2007). However, comparatively slow average rising speed (110 km s^{-1}), steady ballistic motion, the absence of impulsive heating at the base and no gradual enhancement in plasma temperature etc., indicate the role of magnetic reconnection as an indirect mechanism. The jet is seem to be driven by a large amplitude velocity pulse that may be excited non-linearly by recurrent magnetic reconnection at the base of the polar coronal hole. This pulse steepens into a slow shock front which moves at a higher temperature wave front. However, the density and typical emissions are low in polar coronal holes. Therefore, we could not observe high temperature bright front of the jet. Later, the motion of the slow shock, under stable conditions, causes the propagative rarefaction wave which direct the cool and denser chromospheric/TR plasma upward. This steadily moving plasma is clearly visible in the observations as well as in the simulation. After reaching at the height of ~ 75 Mm, the plasma begins to subside. The gravitational free fall plays the role for the falling of jet material. During the subsiding phase of the jet, in the numerical simulation, the another pulse is evident at the base that causes the low rate of subsided plasma compared to the observations. However, the realistic solar atmosphere is rather complex, and there is a possibility that the huge downfalling material causes the vanishing of the another pulses coming from the lower atmosphere. This is the reason why a pulse driven single jet became evident above the limb rather than multiple jets at the same place.

In conclusion we suggest that the initial velocity pulse launched below the transition region is able to trigger a hot plasma shock which is followed by a cool plasma jet. This cold plasma jet approximately resembles many of the features which are found in the presented SDO/AIA observational data. We report first time on the observations of a pulse driven plasma jet in the polar region and provide theoretical explanation of this phenomenon on the basis of numerical simulations we performed. However, further multiwavelength observations should be performed by high-resolution space borne (e.g., SDO, Hinode, STEREO) and complementary ground based observations to shed new light on this kind of unique jets that rise and fall back in the solar atmosphere. This will also impose a rigid con-

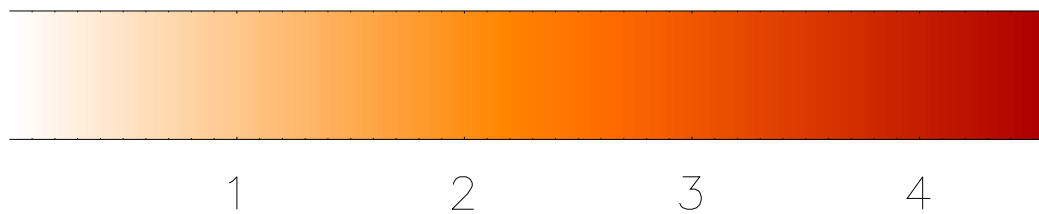
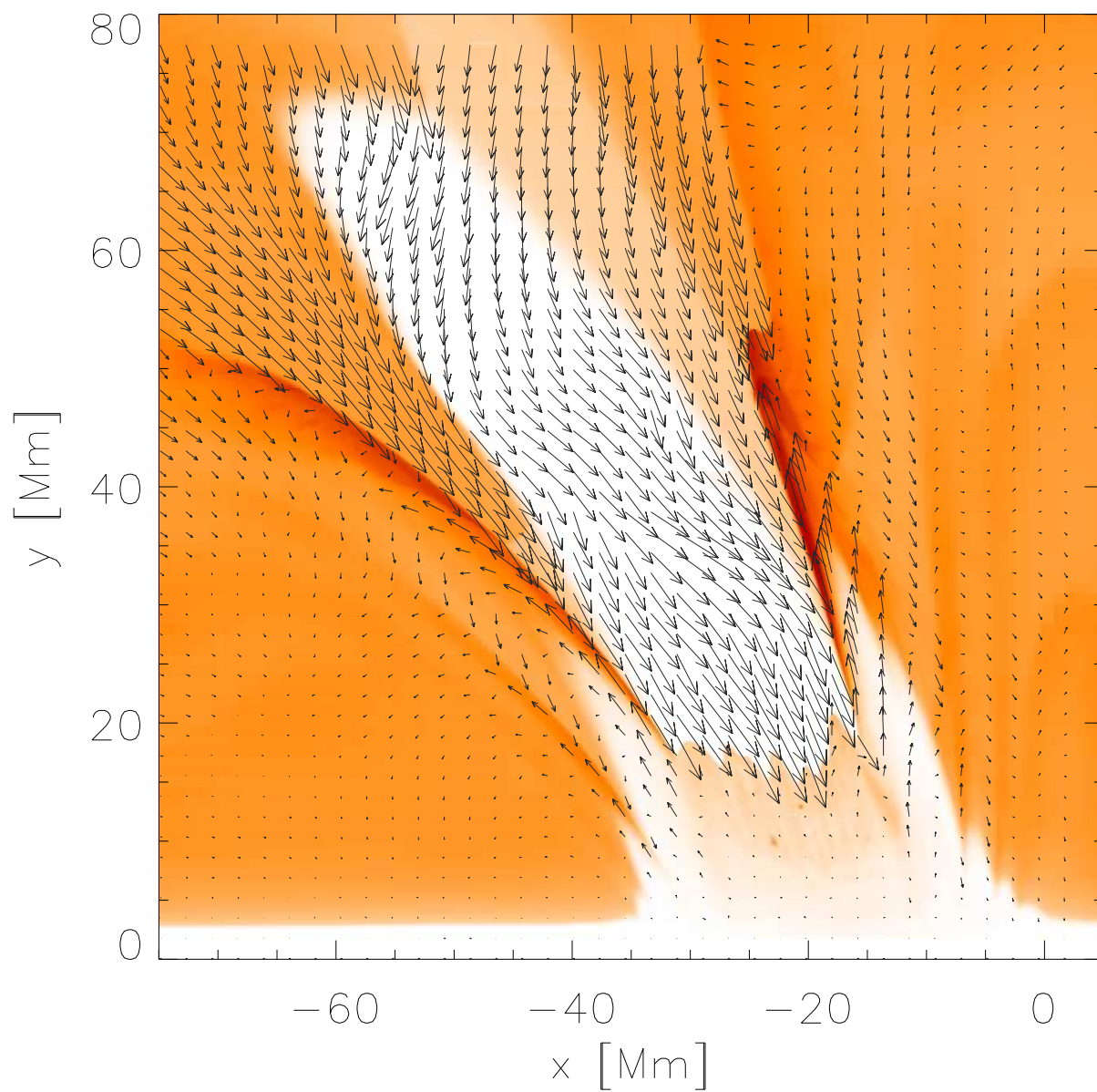
straint on the stringent simulations of such kind of jets in the model solar atmosphere.

6. Acknowledgment

We thank the reviewer for his/her valuable suggestions that improved the manuscript considerably. We acknowledge the use of the SDO/AIA observations for this study. The data is provided courtesy of NASA/SDO, LMSAL, and the AIA, EVE, and HMI science teams. The FLASH code has been developed by the DOE-supported ASC/Alliance Center for Astrophysical Thermonuclear Flashes at the University of Chicago. AKS thanks Shobhna Srivastava for patient encouragements during the work.

References

- Alexander, D. & Fletcher, L. 1999, *Sol. Phys.*, 190, 167
- Bohlin, J. D., Vogel, S. N., Purcell, J. D., et al. 1975, *ApJ*, 197, L133
- Brooks, D. H., Kurokawa, H., & Berger, T. E. 2007, *ApJ*, 656, 1197
- Cirtain, J. W., Golub, L., Lundquist, L., et al. 2007, *Science*, 318, 1580
- Culhane, L., Harra, L. K., Baker, D., et al. 2007, *PASJ*, 59, 751
- De Pontieu, B., Erdélyi, R., & James, S. P. 2004, *Nature*, 430, 536
- De Pontieu, B., Hansteen, V. H., Rouppe van der Voort, L., van Noort, M., & Carlsson, M. 2007a, *ApJ*, 655, 624
- De Pontieu, B., McIntosh, S., & Carlsson, M. et al. 2011, *Science*, 331, 55
- De Pontieu, B., McIntosh, S., Hansteen, V. H., & Carlsson, M. et al. 2007b, *PASJ*, 59, 655
- Filippov, B., Golub, L., & Koutchmy, S. 2009, *Sol. Phys.*, 254, 259
- Georgakilas, A. A., Koutchmy, S., & Alissandrakis, C. E. 1999, *A&A*, 341, 610
- Hansteen, V. H., De Pontieu, B., Rouppe van der Voort, L., van Noort, M., & Carlsson, M. 2006, *ApJ*, 647, L73
- He, J., Marsch, E., Tu, C., & Tian, H. 2009, *ApJ*, 705, L217
- Innes, D. E., Inhester, B., Axford, W. I., & Wilhelm, K. 1997, *Nature*, 386, 811
- Kamio, S., Curdt, W., Teriaca, L., Inhester, B., & Solanki, S. K. 2010, *A&A*, 510, L1+
- Kamio, S., Hara, H., Watanabe, T., et al. 2007, *PASJ*, 59, 757
- Katsukawa, Y., Berger, T. E., Ichimoto, K., et al. 2007, *Science*, 318, 1594
- Ko, Y.-K., Raymond, J. C., Gibson, S. E., et al. 2005, *ApJ*, 623, 519
- Lee, D. & Deane, A. E. 2009, *Journal of Computational Physics*, 228, 952
- Lemen, J. R., Title, A. M., Akin, D. et al. 2011, *A&A*, A8+
- Liu, W., Berger, T. E., Title, A. M., & Tarbell, T. D. 2009, *ApJ*, 707, L37
- Morton, R., Srivastava, A. K., & Erdélyi, R. 2011, *A&A*, submitted
- Murawski, K. & Zaqarashvili, T. V. 2010, *A&A*, 519, A8+
- Nisticó, G., Bothmer, V., Patsourakos, S., & Zimbardo, G. 2009, *Sol. Phys.*, 259, 87
- Pariat, E., Antiochos, S. K., & DeVore, C. R. 2009, *ApJ*, 691, 61
- Shibata, K., Ishido, Y., Acton, L. W., et al. 1992, *PASJ*, 44, L173
- Shibata, K., Nakamura, T., Matsumoto, T., et al. 2007, *Science*, 318, 1591
- Shimojo, M. & Shibata, K. 2000, *ApJ*, 542, 1100
- Vernazza, J. E., Avrett, E. H., & Loeser, R. 1981, *ApJS*, 45, 635
- Wang, Y.-M., Sheeley, Jr., N. R., Socker, D. G. et al. 1998, *ApJ*, 508, 899
- Yokoyama, T. & Shibata, K. 1995, *Nature*, 375, 42
- Yokoyama, T. & Shibata, K. 1996, *PASJ*, 48, 353



0.15